Title: NOx Storage and Reduction Over Copper-based Catalysts. Part 2: $Ce_{0.8}M_{0.2}O_{\delta}$ Supports (M = Zr, La, Ce, Pr or Nd)

Author: Agustín Bueno-López Dolores Lozano-Castelló James A. Anderson

PII: S0926-3373(16)30424-6
DOI: http://dx.doi.org/doi:10.1016/j.apcatb.2016.05.066
Reference: APCATB 14809

To appear in: *Applied Catalysis B: Environmental*

Received date: 11-4-2016
Revised date: 24-5-2016
Accepted date: 27-5-2016

Please cite this article as: Agustín Bueno-López, Dolores Lozano-Castelló, James A.Anderson, NOx Storage and Reduction Over Copper-based Catalysts.Part 2: Ce0.8M0.2Oδ Supports (M=Zr, La, Ce, Pr or Nd), Applied Catalysis B, Environmental http://dx.doi.org/10.1016/j.apcatb.2016.05.066

NOx Storage and Reduction Over Copper-based Catalysts. Part 2: $Ce_{0.8}M_{0.2}O_{\delta}$ Supports (M = Zr, La, Ce, Pr or Nd)

Agustín Bueno-López[1,2*], Dolores Lozano-Castelló[1,2], James A. Anderson[2]

[1]MCMA group. Inorganic Chemistry Department; University of Alicante.

[2]Surface Chemistry and Catalysis Group, Materials and Chemical Engineering, School of Engineering, University of Aberdeen.

[*]Carretera de San Vicente s/n. E03080, Alicante (Spain), Tel.: (+34) 965903400; Fax. (+34) 965903454, http://personal.ua.es/es/agus
email: agus@ua.es

Graphical Abstract

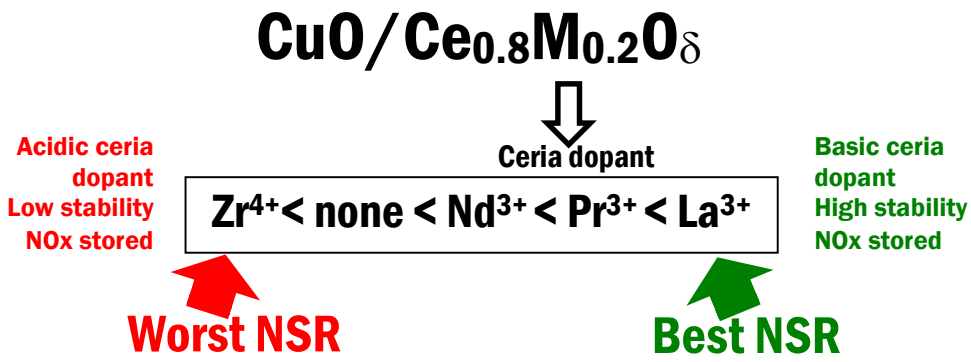

Highlights

- Stored NOx thermal stability depends on the acidic/basic character of the ceria dopant
- Stored NOx thermal stability increases as follows: Zr < none < Nd < Pr < La
- $CuO/Ce_{0.8}La_{0.2}O_{\delta}$: Best NOx removal in NSR experiments with CO + H_2 pulses
- $CuO/Ce_{0.8}Zr_{0.2}O_{\delta}$: Worst NOx removal in NSR experiments with CO + H_2 pulses

Abstract

5% copper catalysts with $Ce_{0.8}M_{0.2}O_{\delta}$ supports (M = Zr, La, Ce, Pr or Nd) have been studied by rapid-scan *operando* DRIFTS for NOx Storage and Reduction (NSR) with high frequency (30 seconds) CO, H_2 and 50%CO + 50%H_2 micropulses. In the absence of reductant pulses, below 200-250ºC NOx was stored on the catalysts as nitrite and nitro groups, and above this temperature nitrates were the main species identified. The thermal stability of the NOx species stored on the catalysts depended on the acid/basic character of the dopant (M more acidic = NOx stored less stable $\Rightarrow$ Zr^{4+}< none < Nd^{3+} < Pr^{3+} < La^{3+} $\Leftarrow$ M more basic = NOx stored more stable). Catalysts regeneration was more efficient with H_2 than with CO, and the CO + H_2 mixture presented an intermediate behavior, but with smaller differences among the series of catalyst than observed using CO alone. N_2 is the main NOx reduction product upon H_2 regeneration. The highest NOx removal in NSR experiments performed at 400ºC with CO + H_2 pulses was achieved with

the catalyst with the most basic dopant ($CuO/Ce_{0.8}La_{0.2}O_{\delta}$) while the poorest performing catalyst was that with the most acidic dopant ($CuO/Ce_{0.8}Zr_{0.2}O_{\delta}$). The poor performance of $CuO/Ce_{0.8}Zr_{0.2}O_{\delta}$ in NSR experiments with CO pulses was attributed to its lower oxidation capacity compared to the other catalysts.

Keywords: NSR; deNOx; diesel aftertreatment; copper catalyst; Ceria; DRIFTS; Operando.

1.- Introduction

Ceria-based oxides are have been used in catalysts for gas pollution control in gasoline vehicles since the beginning of the 1980s [1-4], when they were incorporated into Three Way Catalysts for simultaneous NOx, CO and hydrocarbons abatement. Even at this early stage, researchers realized that the catalytic performance of cerium oxide was improved by doping with other cations such as Zr^{4+}, and Ce-Zr mixed oxides showed higher thermal stability, better reducibility, higher oxygen storage capacity and enhanced oxidation activity compared to cerium oxide alone.

It has been also reported that ceria doping with foreign cations has benefits in other catalytic applications related to gas pollution control in vehicles. Ceria is an excellent catalyst to accelerate soot combustion and regenerate Diesel Particulate Filters (DPF) [5-9]. However, pure ceria sinters readily and losses activity drastically under the highly demanding thermal and chemical operational conditions on these DPFs, and ceria doping with other cations such as those of Zr, Pr or La, among others, is essential in order to achieve suitable thermal stability. Dopants also enhance the production of active oxygen, which is responsible for the high soot oxidation capacity of the ceria-based oxides.

Cerium oxides have been also studied for NOx removal in Diesel exhausts using the NSR technology [9-11], where NOx is stored on the catalyst and a reductant is fed periodically into the exhaust gas stream to reduce the stored NOx species. It has been reported that the NSR performance of Pt/Ceria is improved upon doping ceria with Pr, because Pr accelerates the oxidation of adsorbed NOx species and destabilizes these

species when the reductant is fed [12]. It has been also reported [13] that the thermal stability of Pt/Ceria NSR catalysts is improved by La, Pr and/or Zr doping, and that these materials were active even after hydrothermal aging at 700ºC.

However, to the best of our knowledge, the utilization of copper-based noble metal-free formulations containing solid solutions of ceria with other dopants as NSR catalysts has not been reported, and the goal of the current article is to study this type of materials.

In a previous article [14], copper catalysts were studied by *operando* DRIFTS-MS-Chemiluminiscence in the NSR process using H_2 and CO as reductants, and CeO_2, BaO and BaO + CeO_2 supports were compared. CeO_2 and BaO did not form solid solutions in any appreciable extent, and mixtures of oxides/carbonates were obtained. It was concluded [14] that the copper catalysts with cerium and/or barium oxide/carbonate supports were able to chemisorb NOx at 400ºC, and at this temperature, the general NSR behavior of all catalysts was quite similar. Differences were only observed when using high frequency (30 seconds) pulses of CO, where CuO/CeO_2 showed the best recovery of NOx storage capacity, and NOx chemisorption and desorption rates were faster for CuO/CeO_2 than for CuO/BaO.

The goal of the current article is to report performance of NSR copper catalysts with ceria supports doped with different metal cations, with an aim to improve the NSR performance of CuO/CeO_2. Copper catalysts with $Ce_{0.8}M_{0.2}O_\delta$ supports (M = Zr, La, Ce, Pr or Nd) have been studied by *operando* DRIFTS-MS-Chemiluminiscence. Realistic periods of lean operation (30 seconds) similar to those originally proposed by Toyota in the mid 1990s [15] and periodic micropulses of reductant were used. Rapid-scan DRIFTS was performed in a spectrometer that is able to obtain up to 17 spectra per second.

2.- Experimental details

2.1. Catalysts preparation

$Ce_{0.8}M_{0.2}O_\delta$ supports (M = Zr, La, Ce, Pr or Nd) were prepared with the following precursors: $ZrO(NO_3)_2 \cdot xH_2O$ (Fluka, ~ 27 % Zr), $La(NO_3)_3 \cdot 6H_2O$ (≥ 99.0%),

$Ce(NO_3)_3 \cdot 6H_2O$ (Alfa-Aesar, 99.5 %), $Pr(NO_3)_3 \cdot 6H_2O$ (99.9%) and $Nd(NO_3)_3 \cdot 6H_2O$ (≥ 99.9%).

Aqueous dissolutions of the required precursors were prepared with 10 ml of solvent, using the required amounts to obtain 5 grams of each mixed oxide. The solutions were introduced into a muffle furnace previously heated at 200ºC, and after 1 hour, the temperature increased at 10ºC/min until 500 ºC, holding the samples at this temperature for 2 hours. As previously reported, the $Ce_{0.8}M_{0.2}O_{\delta}$ supports with M = Zr, La, Pr or Nd dopants [16] form mixed oxides where M is located within the parent ceria lattice.

$CuO/Ce_{0.8}M_{0.2}O_{\delta}$ catalysts were prepared with a 5 wt. % target Cu loading. The required amount of $Cu(NO_3)_2 \cdot 5 \cdot (1/2)H_2O$ (Sigma Aldrich, 98 %) was dissolved in 2 ml of water and 2.5 grams of each support was impregnated with this solution. The impregnated supports were heat treated following the same protocol used for the supports preparation, that is, they were introduced in a muffle furnace previously heated at 200ºC, and after 1 hour, the temperature was increased at 10ºC/min until 500ºC, holding this temperature for 2 hours. Details regarding catalyst characterization are reported elsewhere [16], but BET surface area values are included here, and were 60, 40, 58, 35, and 45 m^2/g for catalysts with M = Zr, La, Ce, Pr and Nd, respectively.

2.2. NOx chemisorption and NSR experiments

NOx chemisorption and NSR performance were studied in a Shimadzu (IR Tracer-100) Fourier Transform Infrared Spectrometer with a Harrick reaction cell coupled to a EcoSys-P mass spectrometer and a chemiluminiscence NOx analyzer (Thermo 42H). The sample holder of the DRIFT cell was 6.3 mm diameter with a height of 3.3 mm which was filled with sample (100 mg in the absence of diluent). It is important to note that the infrared spectrum only provides information on the top < 0.2 mm of this sample [17].

The reaction cell was designed to allow the reaction gas mixture (50 ml/min; 850 ppm NOx + 5% O_2 + N_2) to pass through the catalyst bed with the gas exit under the bed.

It is worth mentioning that temperature control and determination in DRIFTS cells is problematic. It has been reported that the actual temperature of the catalyst bed can be

significantly lower than the set temperature, with differences of around 50ºC when operating at 400ºC [18]. This must be kept in mind when cross referring to data obtained using other devices including reactors.

Three types of experiments were carried out: Temperature programmed NOx storage experiments, isothermal NOx storage at 400ºC and Isothermal NOx Storage and Reduction (NSR) at 400ºC.

In temperature programmed NOx storage experiments, the temperature was increased until 150ºC in N_2 flow, and was held at this temperature for 15 min. A background spectrum of the catalyst was recorded at 150ºC in N_2, and then, the inert gas was replaced by $NOx/O_2/N_2$ and the temperature increased at 10ºC/min until 500ºC. DRIFT spectra and chemiluminescence NOx measurements were simultaneously recorded. 33 scans were averaged to obtain each spectrum, which were measured in the range 4000-1000 cm^{-1} at 4 cm^{-1} resolution.

For isothermal NOx storage experiments at 400ºC, the temperature was increased from room temperature to 400ºC under N_2. A background spectrum of the catalyst was recorded at 400ºC, and then the inert gas was replaced by the $NOx/O_2/N_2$ mixture, considering this as time = 0 min. DRIFT spectra and chemiluminescence NOx measurements were simultaneously recorded with time until saturation of the catalysts. In these experiments, the settings used to obtain the spectra were the same as in previous temperature programmed NOx storage experiments.

Isothermal NOx storage and reduction (NSR) experiments were carried out following the protocol described for isothermal NOx storage experiments at 400ºC, but 100 µl pulses of 100 % CO, 100 % H_2 or 50 % CO + 50 % H_2 were additionally fed with frequencies of 30 seconds. This frequency is in the range of realistic values for application of the NSR technology, as developed by Toyota [15,19,20]. In these experiments, the DRIFT spectrometer was operated in the rapid-scan mode, and one DRIFT spectrum was recorded per second as an average of 7 scans, which were recorded with a resolution of 8 cm^{-1} in the 4000-1000 cm^{-1} range. The Rapid-scan Software (Shimadzu Corporation) was used to handle the large volume of data generated. The gas composition was monitored in these experiments with the mass spectrometer. This detection technique was used instead of chemiluminiscence due to the higher sampling frequency of the mass spectrometer, which was more convenient for fast screening during pulse experiments.

Previous comparison of the NOx concentrations measured by chemiluminiscence and mass spectrometry (m/z 30) confirmed that both techniques provide comparable results. The benefit of chemiluminiscence is that is able to distinguish between NO and NO_2 while the m/z 30 signal shows the NOx sum (i.e. = NO + NO_2).

3.- Results and discussion

3.1. Temperature programmed NOx storage experiments

Figure 1 shows the NOx (Figure 1a) and NO_2 (Figure 1b) profiles monitored during temperature programmed experiments with the chemiluminiscence NOx analyzer. All catalysts chemisorbed NOx and oxidized NO to NO_2 in the range of temperatures screened. NOx storage on a NSR catalyst usually depends on its NO oxidation capacity, because NO_2 is more readily chemisorbed than NO, and on the capacity of the NOx storage component. The NO_2 profiles (Figure 1b) obtained with all catalysts are quite similar, and therefore, differences in NOx profiles (Figure 1a) must be mainly attributed to the chemisorption capacity of the $Ce_{0.8}M_{0.2}O_{\delta}$ supports.

The dopant loaded to the ceria support affects both the chemisorption of NOx on the catalysts and the stability of the chemisorbed species. Additionally the acid/basic character of the dopants seems to play a major role while the BET surface area of the catalysts seems to be of less relevance. Among catalysts compared, the lowest NOx chemisorption capacity was obtained with $CuO/Ce_{0.8}Zr_{0.2}O_{\delta}$. This catalyst chemisorbed NOx from 150 to 260ºC (Figure 1a), and the stored NOx species decomposed above 340ºC. The NOx chemisorption capacity of the dopant-free catalyst (CuO/CeO_2) was higher than that of $CuO/Ce_{0.8}Zr_{0.2}O_{\delta}$, and the decomposition of the nitrogen species stored on CuO/CeO_2 took place above 375ºC. The decrease in the NOx chemisorption capacity of CuO/CeO_2 upon Zr^{4+} doping is consistent with the acidic character of this dopant cation with regard to Ce^{4+} (same charge but smaller size), and this acidic character of Zr^{4+} is expected to hinder the interaction of the catalyst with NO and NO_2, as these are also acidic gases. On the other hand, La^{3+}, Pr^{3+} and Nd^{3+} are more basic than Ce^{4+}, and all of these improved NOx storage capacity with regard to CuO/CeO_2 and delayed the release of the stored species to higher temperatures. It is known that the basicity of +3 lanthanide cations (La^{3+}, Pr^{3+} and Nd^{3+}) decreases with the atomic number (more basic $La^{3+} > Pr^{3+} >$

Nd^{3+} less basic). The ionic radii are quite similar for all of these, and due to the internal location of the *4f* electrons, the attraction of the valence electrons by the nuclei increases with the number of protons. This trend in basicity correlates with the behaviour of the catalysts, and, for instance, the onset temperature for decomposition of the NOx species stored on the catalysts (in brackets in ºC and in Table 1) followed the same trend as the acid/basic character of the doping cations:

More acidic Zr^{4+}(340) < none (375) < Nd^{3+} (407) < Pr^{3+} (407) < La^{3+} (444) More basic

The DRIFT spectra recorded during the temperature programmed NOx storage experiments are compiled in Figure 2. The most relevant bands of nitrogen- and carbon-containing species appear in this 1700-1200 cm^{-1} range. All catalysts showed bands related to the formation of nitro, nitrites and nitrates, and the accumulation of these nitrogen species on the catalysts leads to the decomposition of carbonates present on the fresh samples. This was supported by the decrease in intensity of bands around 1480 and 1350 cm^{-1} due to carbonate species [21] as a function of temperature.

Before discussing in detail the behaviour of the different bands due to nitrogen species observed in Figure 2, it is worth mentioning that it has been recently reported that the molar absorption coefficients of the overlapping bands of carbonates and nitrates differ. For this reason, the true position of the nitrate and nitrite bands cannot be assessed in such complex spectra [22, 23]. However, despite this limitation, some general conclusions can be reached bearing in mind that the exact band positions indicated in the discussion may differ to an extent from those described for other carbonate-free systems.

The first nitrogen species detected on the catalysts at low temperature (150ºC) in Figure 2 are bridging nitrites ($(M\text{-}O)_2$=N; band at 1200-1180 cm^{-1}) and nitro groups in some cases ($(M\text{-}NO_2)$; band at 1435 cm^{-1}) [24]. There are different mechanisms of nitrite formation upon NOx chemisorption on ceria, and the most reasonable under the experimental conditions would be the chemisorption of NO on ceria oxygen, where N (II) (NO) is oxidized to N (III) (NO_2^-). An alternative pathway could be the chemisorption of NO on hydroxyl groups, leading to H_2O release, but this option is ruled out due to the absence of DRIFTS evidence for hydroxyl depletion (bands around 3500 cm^{-1}). An additional option to yield nitrites would be the chemisorption of NO_2 (with N^{4+}) on reduced Ce^{3+} sites (to yield N^{3+}). This pathway could occur under experimental conditions

here but with a minor contribution, because NO_2 concentration at 150ºC is much lower than that of NO (Figure 1b) and Ce^{4+} is expected to be much more abundant than Ce^{3+} (the catalysts were calcined at 500ºC and the gas mixture is highly oxidizing). The formation of nitro groups (M-NO_2) could result from NO chemisorption on surface oxygen or the consequence of NO_2 chemisorption on cationic sites.

The increase in temperature leads to the depletion of nitrite bands and to the formation of nitrates, with bands around 1545, 1235 and 1010 cm^{-1} that could be attributed to monodentate (M-O-NO_2) or bidentate nitrates (M-O_2NO) [24]. The presence of dopants affected the onset temperature for nitrate formation. For instance, nitrate bands were observed at 200ºC on CuO/CeO_2 and CuO/$Ce_{0.8}Zr_{0.2}O_{\delta}$ while 250ºC was required for catalysts with La, Pr or Nd. This would suggest that the low temperature oxidation capacity of CuO/CeO_2 and CuO/$Ce_{0.8}Zr_{0.2}O_{\delta}$ is higher than that of the remaining catalysts under the experimental conditions employed here (note that, as it will be discussed below, the opposite has been observed at 400ºC during reductant pulses).

Additional nitrate bands were identified for some catalysts, which means that nitrate configuration could change with temperature. For instance, the shoulder/band at 1600 cm^{-1} observed on CuO/$Ce_{0.8}Zr_{0.2}O_{\delta}$ at 300ºC and higher temperatures is consistent with the formation of bridging nitrates ($(M\text{-}O)_2$=NO).

As a summary, temperature programed experiments showed that the NOx storage capacity and the stability of the NOx species accumulated on the catalysts increases with the basic character of the dopants loaded to ceria, Zr being the most acidic and La the most basic among those studied. The nature of the nitrogen species accumulated on the catalysts depends on temperature, nitrites and nitro groups being formed at low temperature (below 200-250ºC) and nitrates at higher temperatures.

3.2. Isothermal NOx storage at 400ºC.

Isothermal NOx storage experiments were carried out at 400ºC, based on the results of the temperature programmed experiments. As previously mentioned, NOx chemisorption on a NSR catalyst depends both on the NO oxidation capacity and on the NOx storage capacity of the support. 400ºC is the temperature for maximum NO_2 production for all catalysts (Figure 1b), and therefore, the effect of the NO oxidation

capacity on NOx chemisorption can be ruled out, that is, differences in NOx chemisorption at 400ºC can be only attributed to the NOx storage capacity.

Figure 3 shows the NOx removal profiles at 400ºC. All catalysts chemisorbed NOx at this temperature, and the NOx storage capacity was influenced by the selection of the ceria dopant. For instance, CuO/CeO_2 and $CuO/Ce_{0.8}Zr_{0.2}O_\delta$ were saturated after 45 min while $CuO/Ce_{0.8}La_{0.2}O_\delta$ and $CuO/Ce_{0.8}Pr_{0.2}O_\delta$ after 120 min. All basic dopants (La, Pr and Nd) increased the NOx storage capacity of CuO/CeO_2, and this can be attributed to the stronger interaction of the ceria support with the chemisorbed acidic gases. On the other hand, Zr did not improve the NOx storage capacity of CuO/CeO_2, and this is also consistent with the acidic character of the Zr^{4+} cations.

The amounts of NOx stored on the catalysts were calculated and are compiled in Table 1. The amounts stored on the most efficient catalysts (366 $\mu molNOx/g_{catalyst}$ for $CuO/Ce_{0.8}La_{0.2}O_\delta$ and 368 $\mu molNOx/g_{catalyst}$ for $CuO/Ce_{0.8}Pr_{0.2}O_\delta$) are similar to the value reported in the literature for a $1\%Pt–20\%Ba/Al_2O_3$ reference catalyst (324 $\mu molNOx/g_{catalyst}$ at 400ºC; [25]) and half to that reported for a $1\%Pt–10\%Ba/Al_2O_3$ reference catalyst (714 $\mu molNOx/g_{catalyst}$ at 400ºC; [26]). These NOx storage values (in brackets) provide further evidence about the important role of the basicity of the support dopants:

More acidic $Zr^{4+}(166) <$ none $(168) < Nd^{3+}(198) < Pr^{3+}(368) < La^{3+}(366)$ More basic

The nature of the species formed on the catalysts upon NOx chemisorption at 400ºC was monitored by DRIFTS, and the time-resolved spectra obtained for $CuO/Ce_{0.8}Zr_{0.2}O_\delta$ and $CuO/Ce_{0.8}La_{0.2}O_\delta$ as examples are shown in Figure 4, All catalysts showed there bands around 1540, 1220 and 1010 cm^{-1} that can be assigned to monodentate and/or bidentate nitrates, and a small band at 1420 cm^{-1}, which is consistent with the formation of nitro groups [24]. These results confirm the catalytic oxidation of nitrogen from N (II) on NO, which is the main NOx in the fed, mainly to N (V) on nitrates at 400ºC.

Minor differences were found in the time-resolved spectra at 400ºC among catalysts, and only shoulders were detected in some peaks. The most relevant were those observed at 1600 cm^{-1} on $CuO/Ce_{0.8}Zr_{0.2}O_{\delta}$ which can be assigned to bridging nitrate [24].

Despite all catalysts form the same species upon NOx chemisorption at 400ºC, this information is relevant for further comparison with the performance in the NSR tests discussed in the next section, where differences were noticed in the chemisorbed nitrogen species while reductants pulsing.

3.3. Isothermal NOx Storage and Reduction (NSR) at 400ºC.

NOx storage and reduction experiments were performed at 400ºC using pulses of CO, H_2 or 50% CO + 50% H_2 at 30 seconds frequency. The NOx concentrations monitored during the experiments following the m/z = 30 signal are included in Figure 5 for all catalysts.

Over short periods, peaks appear in the m/z 30 profile because of NOx slip, that is, once the reductant pulse was fed, part of the NOx stored on the catalyst was reduced but a fraction was released without undergoing reduction.

Over longer time periods, the trend in the m/z 30 signals depended on which reductant was pulsed and on the nature of the catalyst. For all catalysts, full regeneration was not achieved with pure CO, and the m/z 30 signals increased with time. On the other hand, the m/z 30 decreased when H_2 was fed, indicating that the catalysts were being regenerated and that part of the NOx previously stored during CO pulses were removed by H_2. The better performance of H_2 compared to CO was also previously reported for $Pt/Ba/Al_2O_3$ NSR catalysts [26-28]. Behavior and effectiveness of the mixed CO + H_2 pulses was in between that of CO and H_2, and the catalysts reached stable levels of NOx removed.

The longer-term trend of the NOx concentrations was analyzed in greater detail, by employing a fitting of the m/z 30 signals as shown in the example included in Figure 5c for H_2 pulses. The NOx concentration at the beginning of each pulse was taken for the fitting, and trend lines were obtained. These trend lines are included in Figure 6 after normalization by dividing all data corresponding to each trend line by the NOx concentration of the first point of each series, that is, all trend lines start with a value of

1, and relative changes were plotted. Also, the time scales used in Figure 6 were set by considering time = 0 min at the beginning of the first pulse of each series.

Pure CO was ineffective at regenerating the catalysts (Figure 6a), and all trend lines increased with time. Nevertheless, differences were observed between different samples. Considering the NOx levels at the end of the series (after 15 min), the poorest results were obtained with $CuO/Ce_{0.8}Zr_{0.2}O_{\delta}$ followed by CuO/CeO_2, and the three catalysts with lanthanide dopants (La, Pr and Nd) behaved quite similarly and suffered less significant decreases in their NOx removal capacity with time. The interpretation of these differences are discussed in detail below, analysing the rapid-scan DRIFT spectra. However, a clear trend was that ceria doping with an acidic cation such as Zr^{4+} had a much worse effect on the extent of regeneration in CO than doping with basic cations such as La^{3+}, Pr^{3+} or Nd^{3+}.

The opposite trend was obtained during H_2 regeneration pulses (Figure 6b). H_2 was able to regenerate all catalysts until stable NOx removal levels were achieved, and the most effective catalyst under these experimental conditions was $CuO/Ce_{0.8}Zr_{0.2}O_{\delta}$, followed by CuO/CeO_2 and finally the three catalysts with lanthanide dopants (La, Pr and Nd).

Finally, using the CO + H_2 mixture (Figure 6c) was less effective than pure H_2 alone but much better than pure CO. During the first 10 min of NOx removal under CO + H_2 pulses, the NOx fitting lines increased slightly, but after this time, stable levels were achieved with all catalysts. Differences among catalysts were minor, but it was still possible to distinguish that the catalyst with the most acidic dopant ($CuO/Ce_{0.8}Zr_{0.2}O_{\delta}$) reached the lowest NOx removal level while the catalyst with the most basic dopant ($CuO/Ce_{0.8}La_{0.2}O_{\delta}$) the highest levels.

Rapid-scan DRIFTS is a powerful tool to study the surface of the catalysts during the transient conditions of the NSR experiments. Figures 7, 8 and 9 show plots of the absorbance at selected wavenumbers monitored during pulses of CO, H_2 and CO+H_2 respectively. The profile of the m/z 30 signal has been included in these figures.

3.3.1. Rapid-scan DIRIFTS analysis during NSR experiments with CO pulses.

All catalysts showed nitrate bands during the NSR experiments with CO pulses, and the signal of the maxima absorbance of the band due to nitrates at *ca.* 1556-1500 cm^{-1} is plotted in Figure 7. The other two nitrate bands that are expected to appear around 1250 and 1000 cm^{-1} were also observed, but are excluded for simplicity. The general profile shape of the m/z 30 signal and the nitrates band at 1556-1500 cm^{-1} were quite similar for all catalysts. Once a CO pulse was fed (as indicated by vertical dashed lines) the m/z 30 signal showed a peak due to the NOx slip that occurred together with the reduction. This partially cleaned the catalyst, and the nitrates band intensity dropped to a minimum.

The rapid-scan spectra of the CuO/CeO_2 catalyst only showed bands due to nitrates (Figure 7b), and the position at 1500 cm^{-1} was consistent with the formation of monodentate nitrates. This suggested that the NSR mechanism occurring over CuO/CeO_2 during CO pulses consisted of the chemisorption and subsequent reduction of nitrates (probably monodentate).

On the other hand, the catalysts with ceria dopants showed more complex behavior, which is not surprising because loading of foreign cations is expected to introduce heterogeneity into the chemisorption sites. The band at 1550 cm^{-1} could be attributed to bidentate nitrates, and the bands around 1485-1470 cm^{-1} could be assigned to monodentate nitrates. That is, the CuO/CeO_2 catalyst chemisorbed NOx leading to only one type of nitrate, while the doped catalysts were able to store nitrates of different configurations. The $CuO/Ce_{0.8}La_{0.2}O_{\delta}$ catalyst (Figure 7e) was the only one showing a band at 1360 cm^{-1}, and this feature, together with that at 1463 cm^{-1} could be assigned to carbonates.

The key point to explain the poor NSR behavior of the $CuO/Ce_{0.8}Zr_{0.2}O_{\delta}$ catalyst (Figure 6a) with CO pulses could be the formation of a species as detected by a band at 1438 cm^{-1}, which was only observed for this catalyst (Figure 7a). This band may be assigned to monodentate nitrites, the formation of which would suggest that the oxidation capacity of $CuO/Ce_{0.8}Zr_{0.2}O_{\delta}$ under CO-NSR conditions was poorer than the remaining catalyst, leading to the least effective NOx removal after some time in reaction.

3.3.2. Rapid-scan DIRIFTS analysis during NSR experiments with H_2 pulses.

The absorbance of relevant bands monitored by rapid-scan DRIFTS during the NSR experiments with H_2 pulses are plotted in Figure 8 together with the m/30 (NOx) and 28 (N_2) signals. The pulses of H_2 clean the catalysts surface and lead to NOx and N_2 release. These m/z 30 and 28 profiles confirm that a major proportion of the NOx stored on the catalysts is reduced to N_2 and that few NOx slips. It is worth noting that evidences of other reduction byproducts, like N_2O (m/z 44) or NH_3 (m/z 17) were not observed upon H_2 pulses. Unfortunately, this high selectivity towards N_2 formation as a NOx reduction product observed for H_2 pulses was not confirmed for CO pulses, because both CO and N_2 contribute to the m/z 28 signal impeding monitoring of N_2.

All catalysts showed nitrate bands, and their absorbance at 1550-1500 cm^{-1} is plotted. In accordance with observations in CO-NSR experiments, the position of the nitrate bands for the CuO/CeO_2 catalyst during H_2 pulses (Figure 8b, 1500 cm^{-1}) is consistent with the presence of monodentate nitrates, while the frequency of bands for the doped catalysts (around 1550 cm^{-1}) would suggest the formation of bidentate nitrates.

The catalysts with lanthanide dopants (La, Pr and Nd; Figures 8e, 8d and 8c respectively) only showed bands due to bidentate nitrates, while the $CuO/Ce_{0.8}Zr_{0.2}O_\delta$ (Figure 8a) and CuO/CeO_2 (Figure 8b) catalysts presented more complex spectra. $CuO/Ce_{0.8}Zr_{0.2}O_\delta$ (Figure 8a) additionally involved nitrites (band at 1438 cm^{-1}) and monodentate nitrates (band at 1485 cm^{-1}), but in this case, the low oxidation capacity of $CuO/Ce_{0.8}Zr_{0.2}O_\delta$ as deduced from the presence of such nitrites seems largely irrelevant for NOx removal, because $CuO/Ce_{0.8}Zr_{0.2}O_\delta$ was the most effective catalyst removing NOx in H_2 pulse experiments (Figure 6b). The more effective regeneration achieved with H_2 with respect to CO would mask other effects.

The absorbance of the hydroxyls band at 3615-3605 cm^{-1} only changes for the $CuO/Ce_{0.8}Zr_{0.2}O_\delta$ (Figure 8a) and CuO/CeO_2 (Figure 8b) catalysts. Hydroxyls could be formed by H_2O (H_2 oxidation product) chemisorption on reduced sites of ceria. It is known that hydroxyls are suitable chemisorption sites for NOx, but it seems that this is not occurring in these experiments (Figures 8a and 8b). If NOx were chemisorbed on hydroxyls, the hydroxyls and nitrite/nitrate bands should follow opposite trends, and this is not the case. The nitrites, nitrates and hydroxyls bands follow the same patterns, and this means that all these species are formed and depleted simultaneously. One hypothesis to explain this would be that NOx and H_2O compete for the chemisorption sites of the

catalysts once they are available after the H_2 pulse. H_2O is more basic than NOx, and this would explain why H_2O is not chemisorbed on catalysts with basic dopants (Pr, Nd or La; Figures 8e, 8d and 8c respectively) but only on $CuO/Ce_{0.8}Zr_{0.2}O_{\delta}$ (Figure 8a), and CuO/CeO_2 (Figure 8b). Also, the peaks shapes of the absorbance band due to nitrates (Figure 8a and 8b) are much narrower and sharper than those obtained for catalysts with basic dopants (La, Pr and Nd; Figures 8e, 8d and 8c respectively), and this indicates that regeneration of $CuO/Ce_{0.8}Zr_{0.2}O_{\delta}$ and CuO/CeO_2 by H_2 is much more effective than regeneration of La, Pr or Nd containing catalysts. This better regeneration would explain the best performance by $CuO/Ce_{0.8}Zr_{0.2}O_{\delta}$, followed by CuO/CeO_2, observed in Figure 6b and also that H_2O is more likely to become chemisorbed on these two catalysts.

In conclusion, H_2 is more effective than CO in regenerating all catalysts, and sample containing the acidic dopant ($CuO/Ce_{0.8}Zr_{0.2}O_{\delta}$) is regenerated by H_2 better than those with more basic dopants (La, Pr and Nd).

3.3.3. Rapid-scan DIRIFTS analysis during NSR experiments with CO + H_2 pulses.

Rapid scan DRIFTS monitoring indicated that the catalysts during NSR experiments with CO + H_2 pulses (Figure 9) show some features of H_2-NSR and others of CO-NSR.

The $CuO/Ce_{0.8}Zr_{0.2}O_{\delta}$ catalyst showed DRIFTS bands (Figure 9a) consistent with the participation of monodentate (1485 cm^{-1}) and bidentate (1556 cm^{-1}) nitrates, monodentate nitrites (1435 cm^{-1}) and hydroxyls (3615 cm^{-1}). As deduced from experiments performed with individual reductants, the participation of nitrites could be related to the poorer oxidation activity of this catalyst, and this had a negative effect on the CO-NSR but not on the H_2-NSR. The lower oxidation capacity of $CuO/Ce_{0.8}Zr_{0.2}O_{\delta}$ also affected the behaviour while using pulses of CO + H_2 (Figure 6c), and would explain the lowest extent of NOx removal achieved with this catalyst.

The changes in the absorbance bands due to hydroxyls on $CuO/Ce_{0.8}Zr_{0.2}O_{\delta}$ and CuO/CeO_2 during CO + H_2 pulses (Figure 9a and 9b respectively) are less significant than those observed with pure H_2 pulses (Figure 8a and 8b) due to the lesser amount of H_2 involved. On the other hand, and in accordance with the experiment performed with pure

CO, in experiments with CO + H_2 pulses, the CuO/$Ce_{0.8}La_{0.2}O_\delta$ catalyst was the only one showing a band at 1360 cm^{-1} due to carbonates.

In conclusion, the regeneration of the catalysts with the CO + H_2 mixture (Figure 6c) presented intermediate behavior between CO-NSR (Figure 6a) and H_2-NSR (Figure 6b), with similarities to the NOx removal trends observed with pure CO pulses but with smaller differences amongst catalysts. The rapid–scan DRIFTS monitoring confirms this intermediate behavior in the CO + H_2 mixture.

4.- Conclusions.

Copper catalysts with $Ce_{0.8}M_{0.2}O_\delta$ supports (M = Zr, La, Ce, Pr or Nd) were studied by *operando* rapid-scan DRIFTS for NSR with high frequency (30 seconds) CO, H_2 and CO + H_2 micropulses, and the following conclusions can be drawn:

- In the absence of reductant pulses, NOx was stored on the catalysts as nitrite and nitro groups below 200-250ºC, and above this temperature nitrites were not identified and nitrates were the predominant species. The thermal stability of the NOx species stored on the catalyst showed a dependence on the acid/basic character of M,:

  More acidic/less stable Zr^{4+} < none < Nd^{3+} < Pr^{3+} < La^{3+} More basic/more stable

- The regeneration of the catalysts in the NSR experiments was better with H_2 than with CO, and the CO + H_2 mixture presented an intermediate behavior with the NOx removal trends observed with pure CO pulses but with smaller differences among catalysts. N_2 is the main NOx reduction product upon H_2 regeneration.

- The best NOx removal in NSR experiments performed at 400ºC with CO + H_2 pulses was achieved with the catalyst with the most basic dopant (CuO/$Ce_{0.8}La_{0.2}O_\delta$) while the poorest NOx removal level was achieved with the catalyst with the most acidic dopant (CuO/$Ce_{0.8}Zr_{0.2}O_\delta$).

- In comparison to catalysts with basic dopants (La, Pr and Nd), the poor behavior of the CuO/$Ce_{0.8}Zr_{0.2}O_\delta$ catalyst in NSR experiments with CO pulses was

attributed to its lower NO oxidation capacity under these conditions. $CuO/Ce_{0.8}Zr_{0.2}O_{\delta}$ yielded both nitrites (N (III)) and nitrates (N (V)) upon NOx chemisorption in NSR experiments with CO pulses while the other catalysts did not yield nitrites, but only nitrates (N (V)).

Acknowledgements

The authors thank the financial support of Generalitat Valenciana (Project PROMETEOII/2014/010 and grant BEST/2014/250), the Spanish Ministry of Economy and Competitiveness (Projects CTQ2015-67597-C2-2-R, MAT2014-61992-EXP, and grant PRX14/00249), and the UE (FEDER funding). We thank Dr. A. J. McCue (University of Aberdeen) for support involving the experimental set-up.

References

[1] G. Kim. Ind. Eng. Chem. Prod. Res. Dev. 21 (1982) 267-274.

[2] J. Kaspar, P. Fornasiero, M. Graziani. Catal. Today 50 (1999) 285-298.

[3] A. Trovarelli, C. De Leitenburg, M Boaro, G. Dolcetti. Catal. Today 50 (1999) 353-367.

[4] H.S. Gandhi, G.W. Graham, R.W. McCabe. J. Catal. 216 (2003) 433-442.

[5] U. Hoffmann, T. Rieckmann Chem. Eng. Technol. 17 (1994) 149-160.

[6] J.P.A. Neeft, M. Makkee, J.A. Moulijn. Fuel Proc. Technol. 47 (1996) 1-69.

[7] E. Aneggi, E., C. de Leitenburg, G. Dolcetti, A. Trovarelli. Catal. Today 114 (2006) 40-47.

[8] A. Bueno-López. 146 (2014) 1– 11.

[9] R. Strobel, F. Krumeich, S.E. Pratsinis, A. Baiker. J. Catal. 243 (2006) 229-238.

[10] M. Casapua, J.-D. Grunwaldt, M. Maciejewski, F. Krumeich, A. Baiker, M. Wittrock, S. Eckhoff. Appl. Catal. B 78 (2008) 288–300.

[11] L. Masdrag, X. Courtoisa, F. Cana, B. Cartoixa, S. Raux, A. Frobert, D. Duprez. Catal. Today 241 (2015) 125–132.

[12] V. Rico-Pérez, A. Bueno-López, D. J. Kim, Y. Ji, M. Crocker. Appl. Catal. B 163 (2015) 313–322.

[13] E. Rohart, V. Bellière-Baca, V. Harlé, C. Pitois. SAE Technical Paper 2008-01-0450 (2008) doi:10.4271/2008-01-0450.

[14] A. Bueno-López, D. Lozano-Castelló, J. A. Anderson. NOx Storage and Reduction over Copper-based Catalysts. Part 1: BaO + CeO_2 Supports. Submitted.

[15] N. Takahashi, H. Shinjoh, T. Iijima, T. Suzuki, K. Yamazaki, K. Yokota, H. Suzuki, N. Miyoshi, S. Matsumoto, T. Tanizawa, T. Tanaka, S. Tateishi, K. Kasahara, Catal. Today 27 (1996) 63–69.

[16] A. Davó-Quiñonero, M. Navlani-García, D. Lozano-Castelló, A. Bueno-López, J. A. Anderson. ACSCatal. 6 (2016) 1723−1731.

[17] C. Mondelli, V. Dal Santo, A. Trovarelli, M. Boaro, A. Fusi, R. Psaro, S. Recchia. Catal. Today 113 (2006) 81-86.

[18] H. Li, M. Rivallan, F. Thibault-Starzyk, A. Travert, F.C. Meunier. Phys.Chem. Chem. Phys. 15 (2013) 7321-7327.

[19] J. P. Breen, C. Rioche, R. Burch, C. Hardacre, F. C. Meunier. Appl. Catal. B 72 (2007) 178-186.

[20] J.P. Breen, R. Burch, C. Fontaine-Gautrelet, C. Hardacre, C. Rioche. Appl. Catal. B 81 (2008) 150-159.

[21] D. Gamarra, A. Martínez-Arias. J. Catal. 263 (2009) 189–195.

[22] J. Dupré, P. Bazin, O. Marie, M. Daturi, X. Jeandel, F. Meunier. Appl. Catal. B 181 (2016) 534–541.

[23] J. Dupré, P. Bazin, O. Marie, M. Daturi, X. Jeandel, F. Meunier. Appl. Catal. B 160–161 (2014) 335–343.

[24] K.I. Hadjiivanov. Catal. Rev. Sci. Eng. 42 (2000) 71–144.

[25] L. Lietti, P. Forzatti, I. Nova, E. Tronconi. J. Catal. 204 (2001) 175–191.

[26] Z. Liu, J. A. Anderson. J. Catal., 224 (2004) 18-27.

[27] D. James, E. Fourré, M. Ishii, M. Bowker. Appl. Catal. B 45 (2003) 147–159.

[28] T. Szailer, J. H. Kwak, D. H. Kim, J. C. Hanson, Charles H.F. Peden, J. Szanyi. J. Catal. 239 (2006) 51–64.

Figure captions

Figure 1. NOx concentration (a) and NO_2 percentage with regard to total NO + NO_2 (b) monitored with the chemiluminiscence NOx analyzer during the Temperature Programmed NOx Storage experiments.

Figure 2. DRIFT spectra monitored during the Temperature Programmed NOx Storage experiments with (a) $CuO/Ce_{0.8}Zr_{0.2}O_{\delta}$, (b) CuO/CeO_2, (c) $CuO/Ce_{0.8}Nd_{0.2}O_{\delta}$, (d) $CuO/Ce_{0.8}Pr_{0.2}O_{\delta}$, (e) $CuO/Ce_{0.8}La_{0.2}O_{\delta}$.

Figure 3. NOx removal monitored with the chemiluminiscence NOx analyzer in isothermal experiments at 400ºC.

Figure 4. DRIFT spectra monitored during isothermal experiments at 400ºC with (a) $CuO/Ce_{0.8}Zr_{0.2}O_{\delta}$ and (b) $CuO/Ce_{0.8}La_{0.2}O_{\delta}$.

Figure 5. m/z 30 signal (NOx) monitored during NSR experiments performed with (a) $CuO/Ce_{0.8}Zr_{0.2}O_{\delta}$, (b) CuO/CeO_2, (c) $CuO/Ce_{0.8}Nd_{0.2}O_{\delta}$, (d) $CuO/Ce_{0.8}Pr_{0.2}O_{\delta}$, (e) $CuO/Ce_{0.8}La_{0.2}O_{\delta}$.

Figure 6. NOx data of Figure 5 fitting. NOx concentration at the beginning of each pulse was taken for the fitting, and concentrations were normalized by dividing all data of each series by the NOx concentration of the first point of the series. The time scales were set considering time = 0 at the beginning of the first pulse of each series. (a) CO pulses, (b) H_2 pulses and (c) CO + H_2 pulses.

Figure 7. m/z 30 (NOx) and absorbance at selected wavenumbers monitored during NSR experiments with CO pulses by fast DRIFTS screening for (a) CuO/$Ce_{0.8}Zr_{0.2}O_\delta$, (b) CuO/CeO_2, (c) CuO/$Ce_{0.8}Nd_{0.2}O_\delta$, (d) CuO/$Ce_{0.8}Pr_{0.2}O_\delta$, (e) CuO/$Ce_{0.8}La_{0.2}O_\delta$. Vertical dashed lines indicate when a CO pulse was introduced.

Figure 8. m/z 30 (NOx), 28 (N_2) and absorbance at selected wavenumbers monitored during NSR experiments with H_2 pulses by fast DRIFTS screening for (a) CuO/$Ce_{0.8}Zr_{0.2}O_\delta$, (b) CuO/CeO_2, (c) CuO/$Ce_{0.8}Nd_{0.2}O_\delta$, (d) CuO/$Ce_{0.8}Pr_{0.2}O_\delta$, (e) CuO/$Ce_{0.8}La_{0.2}O_\delta$. Vertical dashed lines indicate when a H_2 pulse was introduced. The baseline of the m/z 28 signal has been subtracted before plotting.

Figure 9. m/z 30 (NOx) and absorbance at selected wavenumbers monitored during NSR experiments with CO + H_2 pulses by fast DRIFTS screening for (a) CuO/$Ce_{0.8}Zr_{0.2}O_\delta$, (b) CuO/CeO_2, (c) CuO/$Ce_{0.8}Nd_{0.2}O_\delta$, (d) CuO/$Ce_{0.8}Pr_{0.2}O_\delta$, (e) CuO/$Ce_{0.8}La_{0.2}O_\delta$. Vertical dashed lines indicate when a CO + H_2 pulse was introduced.

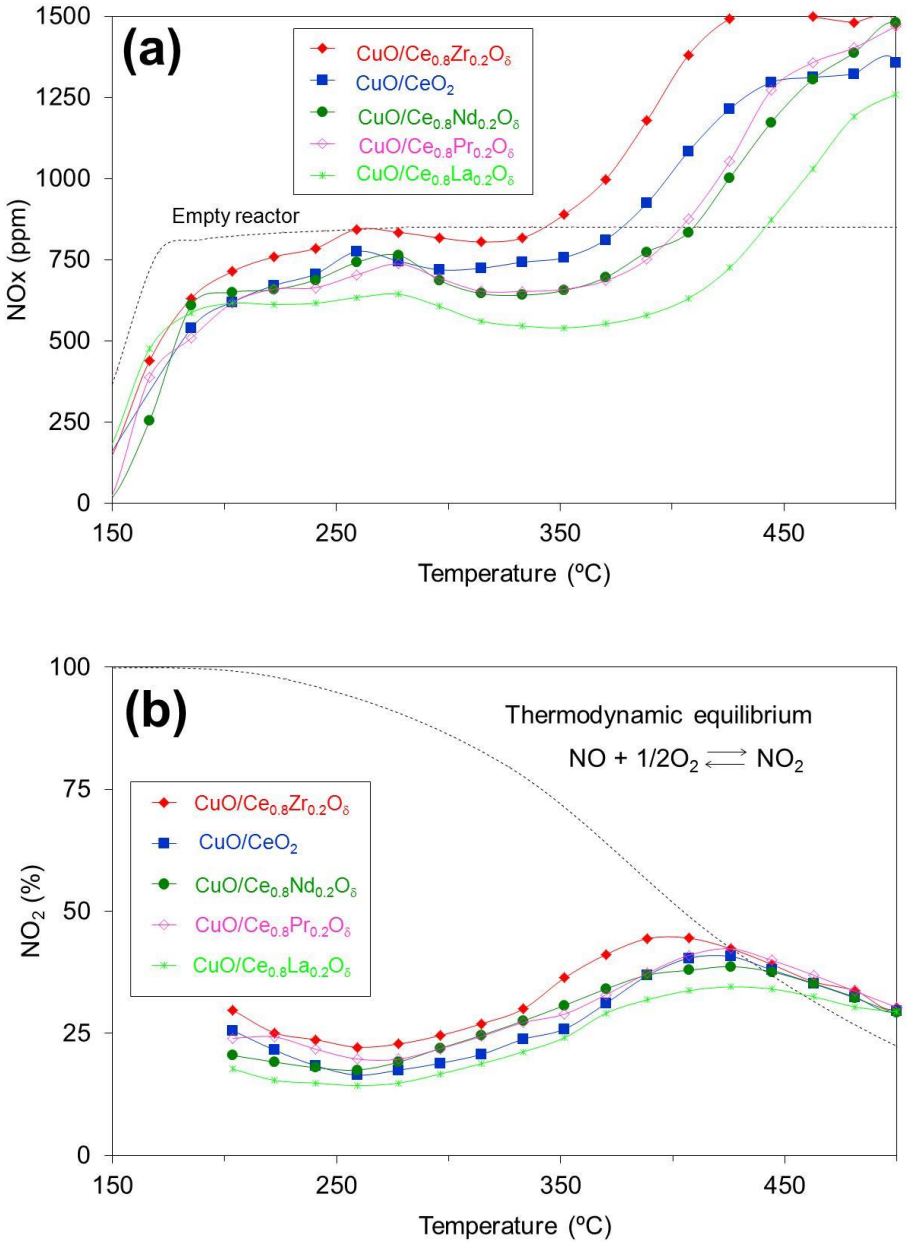

FIGURE 1

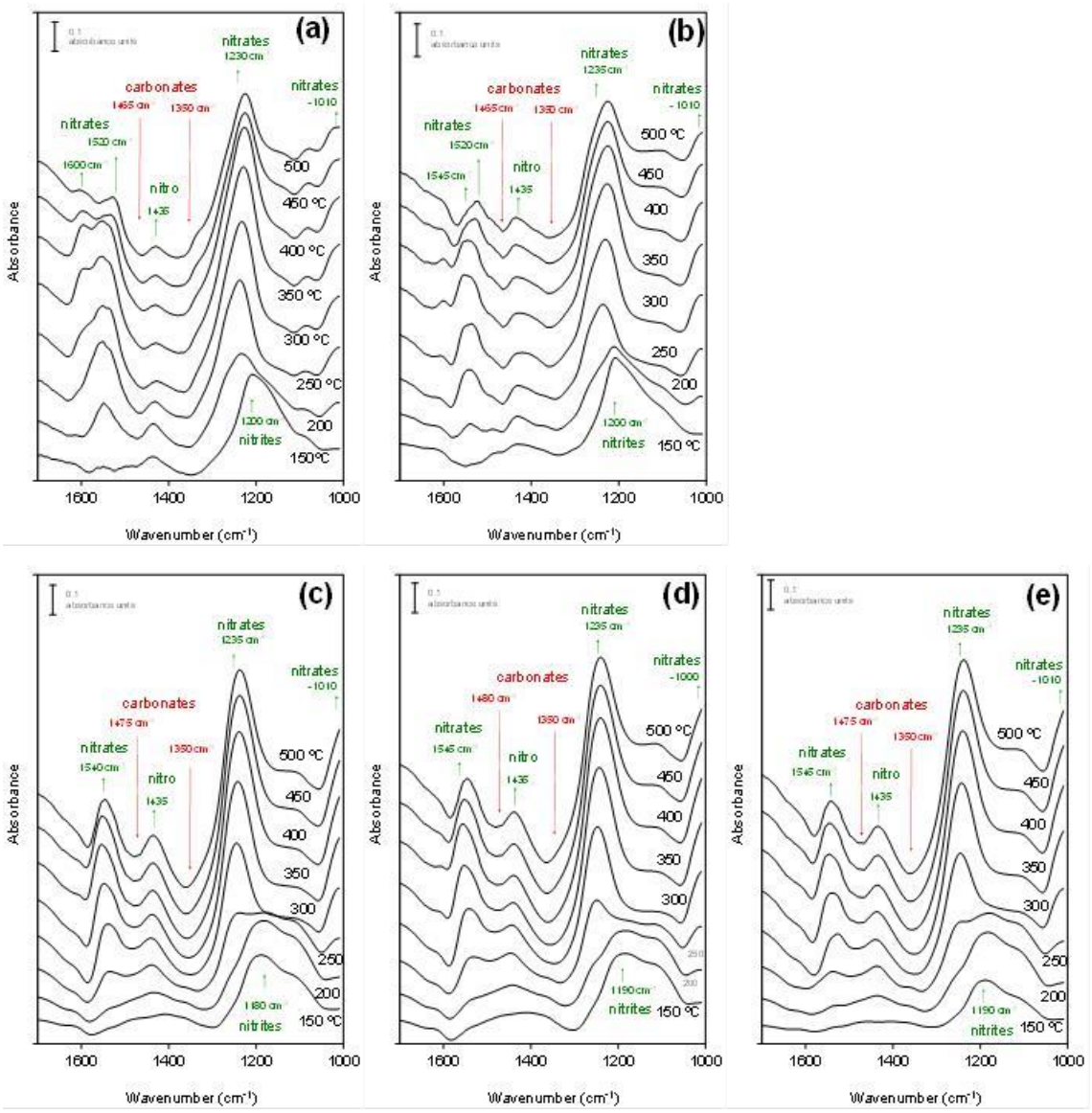

FIGURE 2

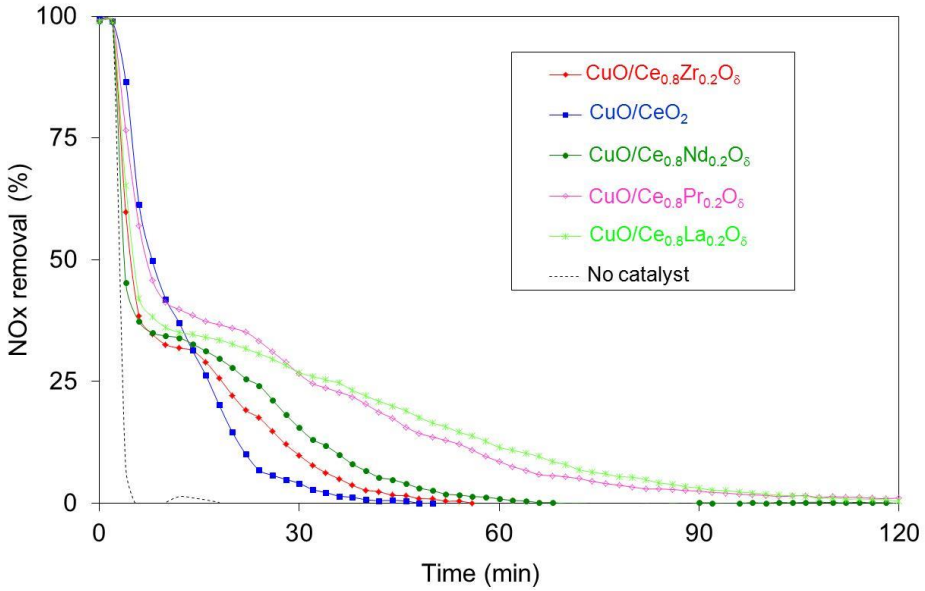

FIGURE 3

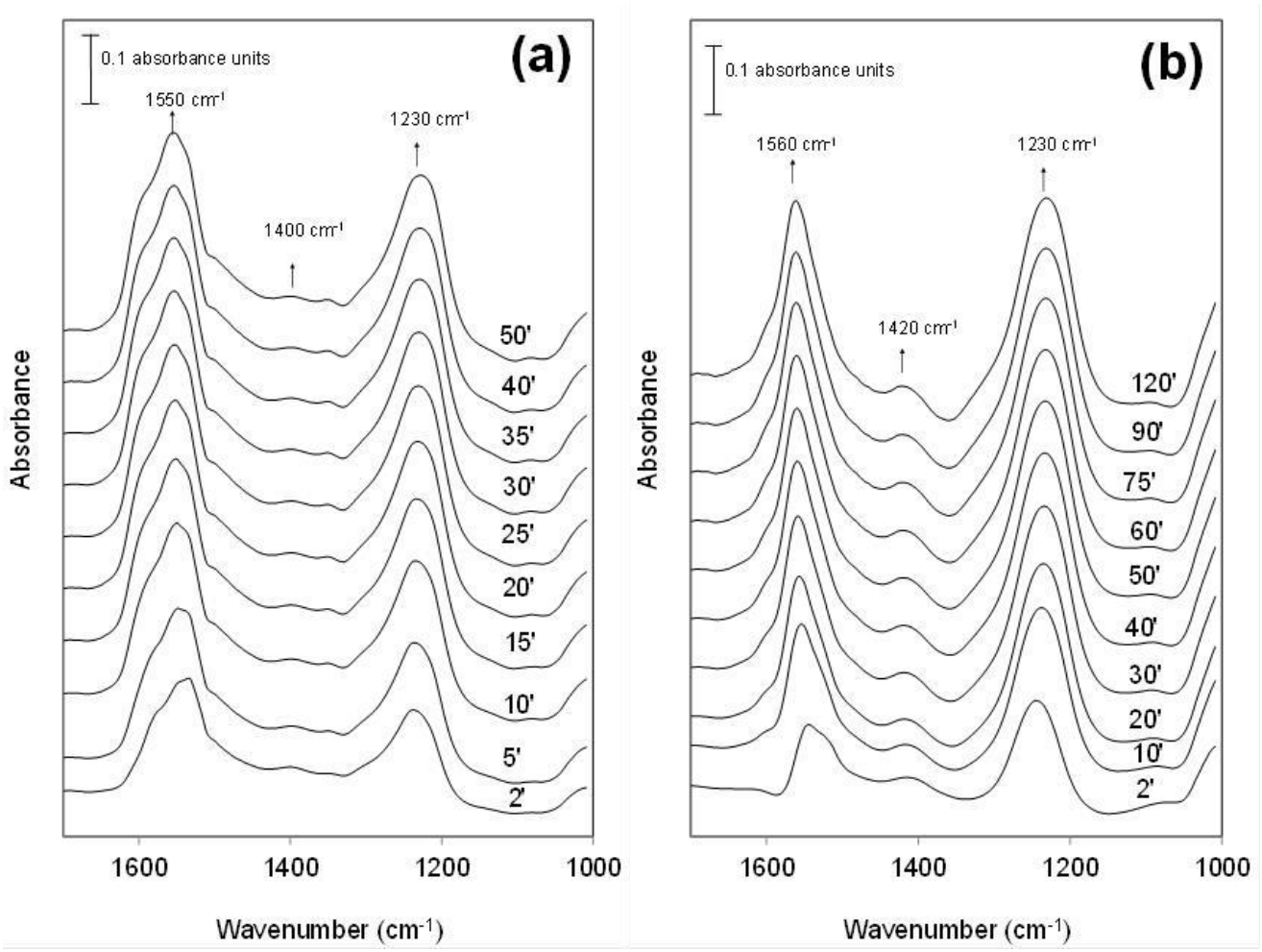

FIGURE 4

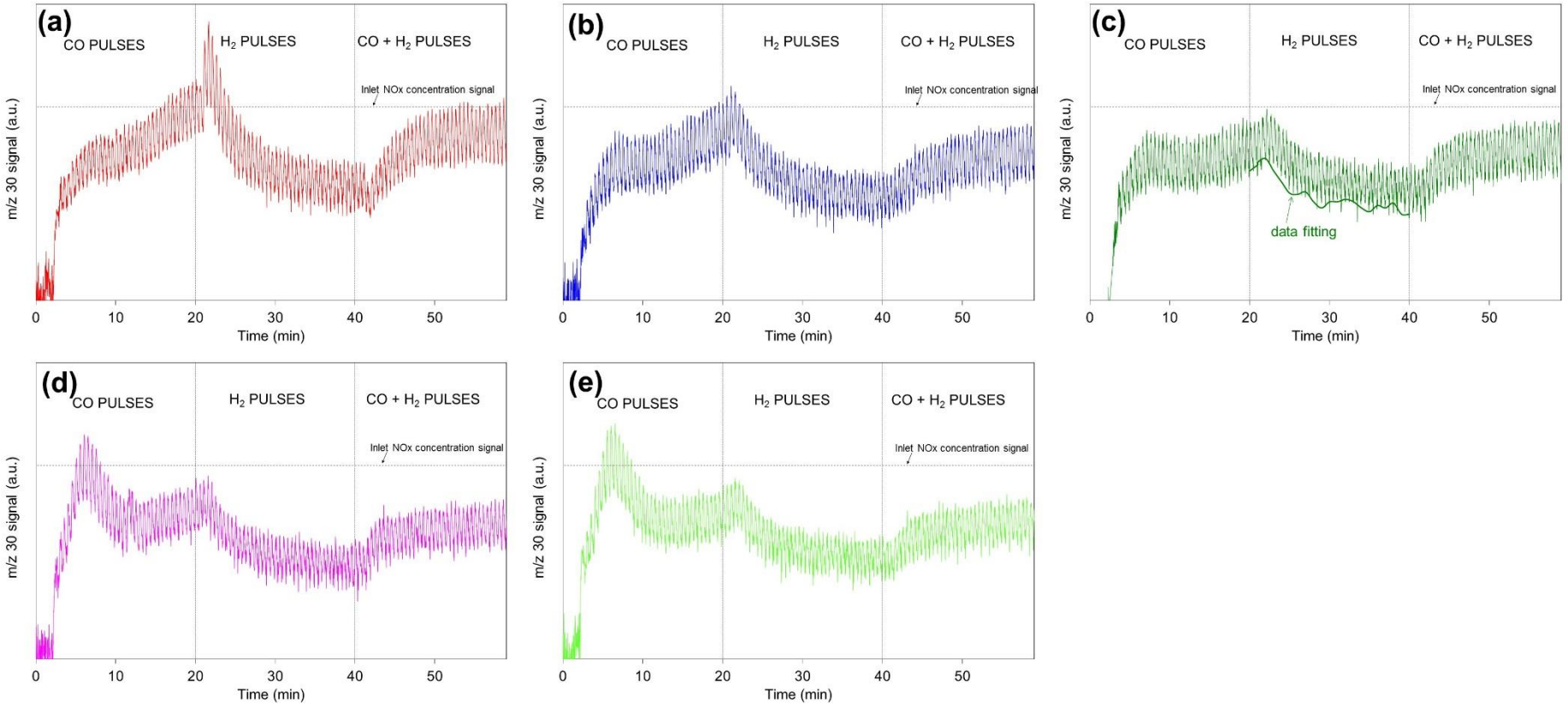

FIGURE 5

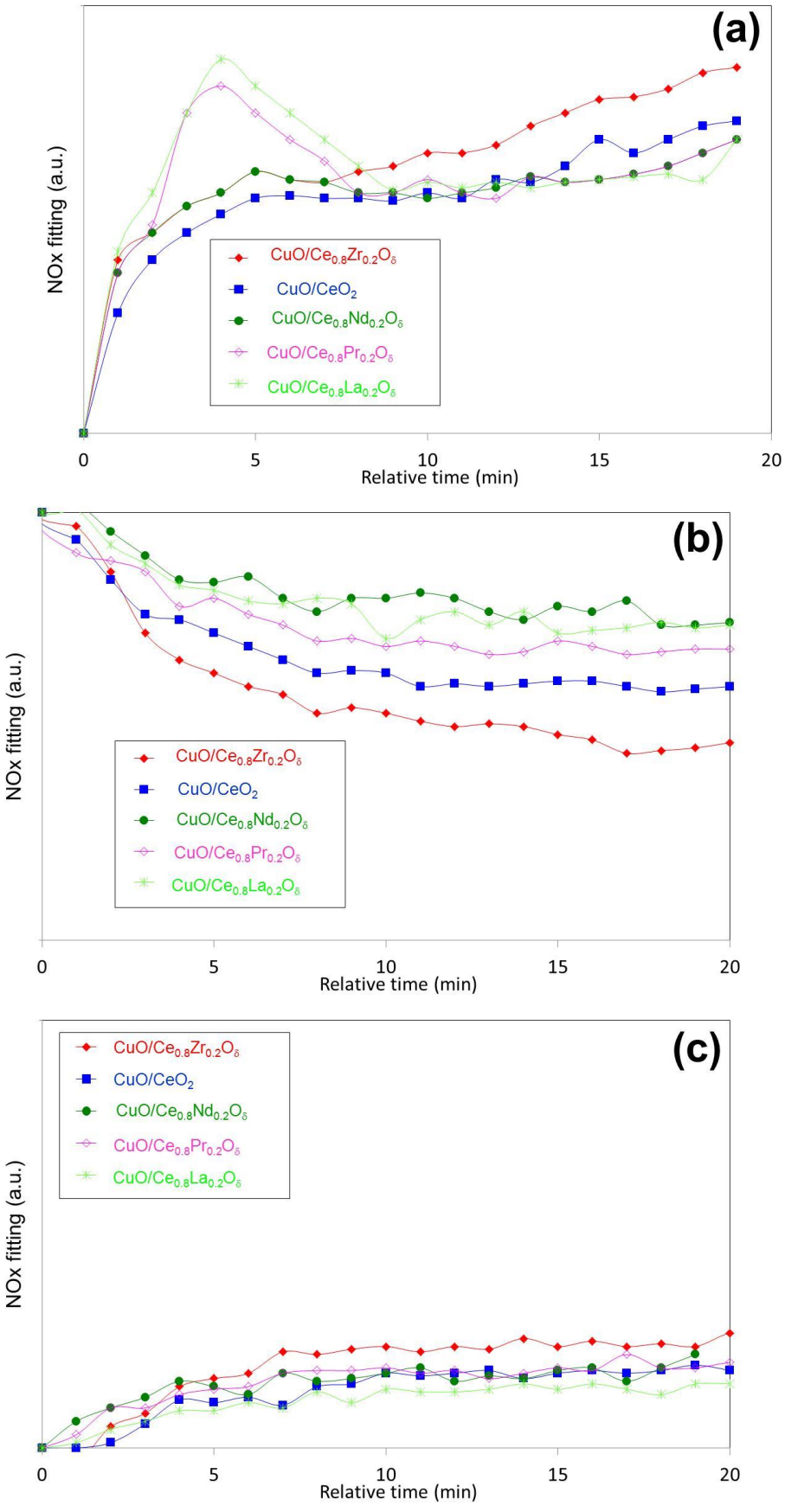

FIGURE 6

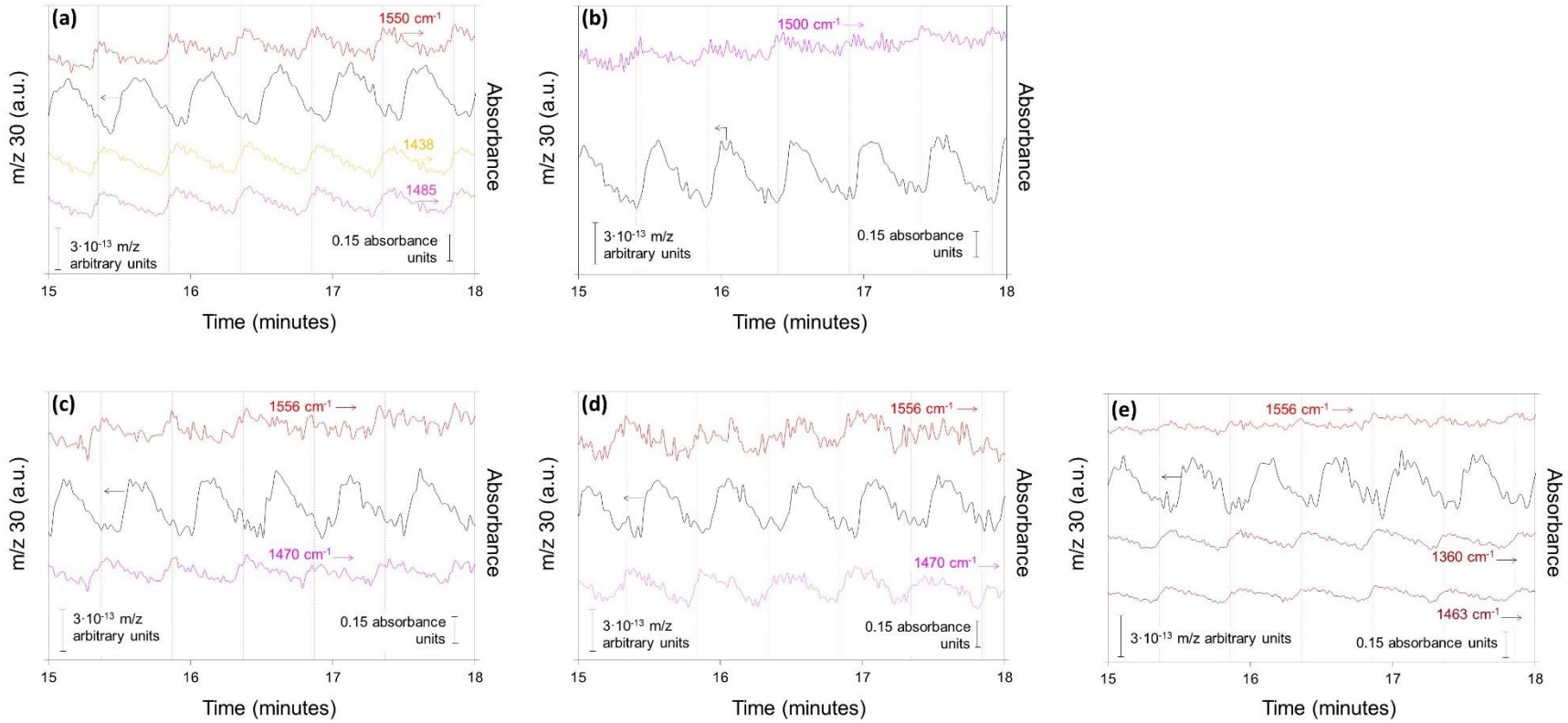

FIGURE 7

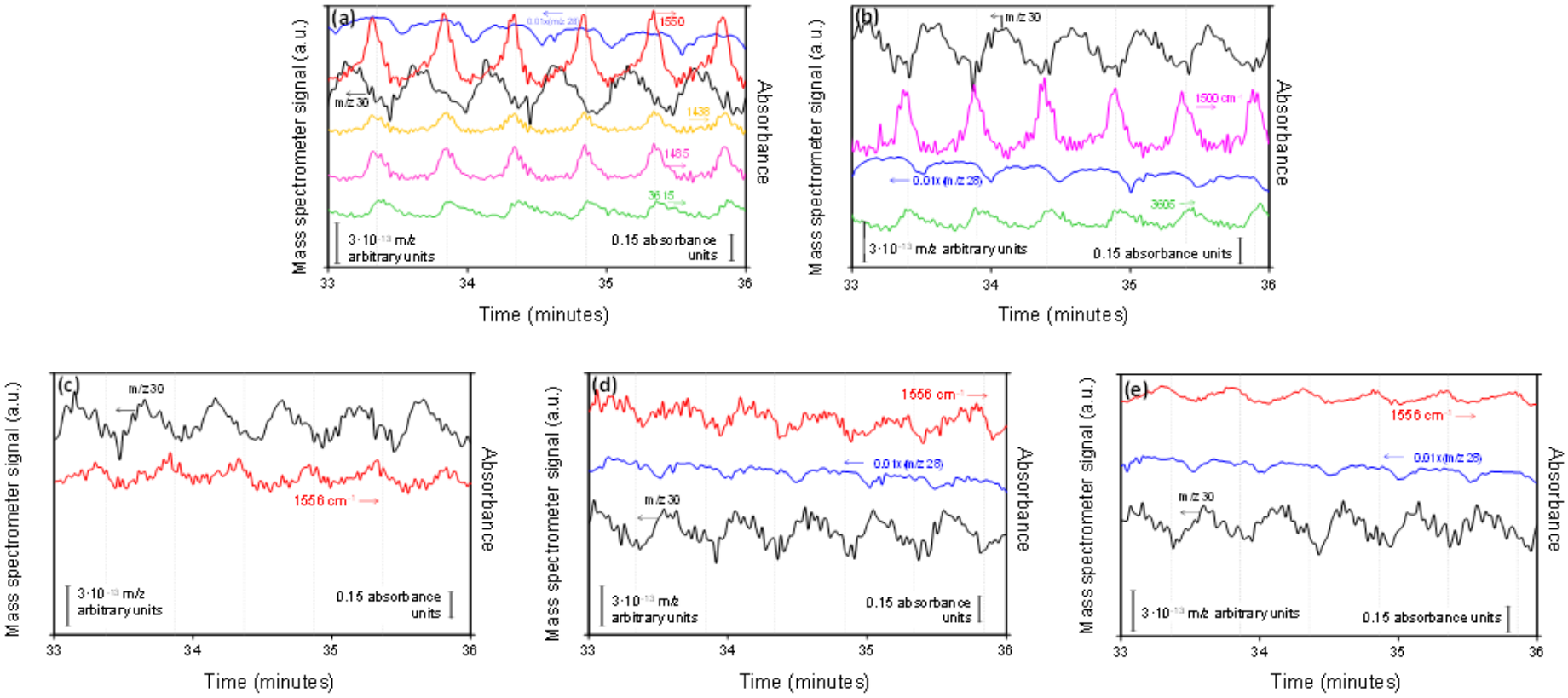

FIGURE 8

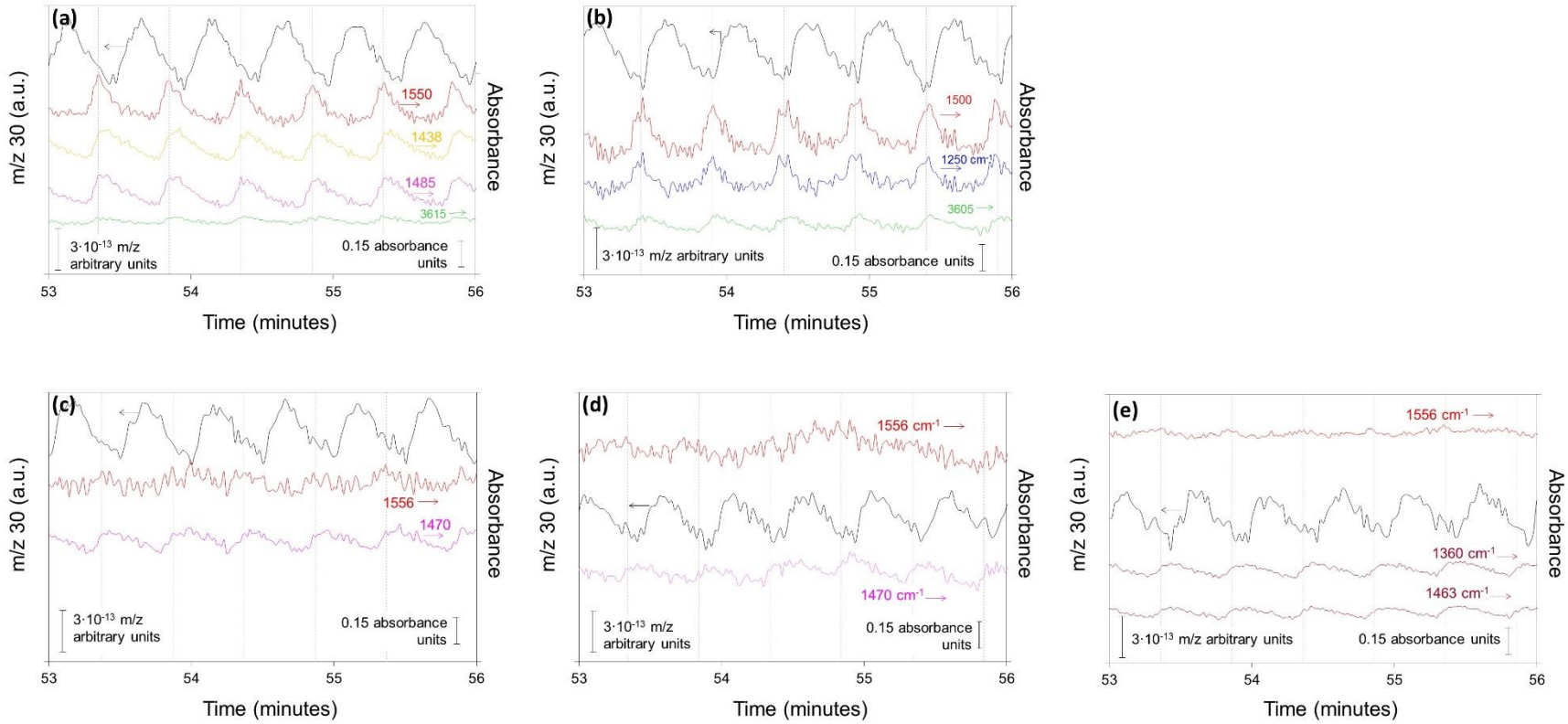

FIGURE 9

Table 1. Onset temperature for NOx decomposition in temperature programmed experiments and amount of NOx stored on the catalysts at 400ºC.

	Onset decomposition temperature (ºC)	NOx stored at 400ºC ($\mu molNOx/g_{catalyst}$)
$CuO/Ce_{0.8}Zr_{0.2}O_{\delta}$	340	166
CuO/CeO_2	375	168
$CuO/Ce_{0.8}Nd_{0.2}O_{\delta}$	407	198
$CuO/Ce_{0.8}Pr_{0.2}O_{\delta}$	407	368
$CuO/Ce_{0.8}La_{0.2}O_{\delta}$	444	366